Global Ecology and Conservation 21 (2020) e00811

Contents lists available at ScienceDirect

Global Ecology and Conservation

journal homepage: http://www.elsevier.com/locate/gecco

Original Research Article

Modeling land cover change based on an artificial neural network for a semiarid river basin in northeastern Brazil

Leonardo Pereira e Silva [a], Ana Paula Campos Xavier [a], Richarde Marques da Silva [b], Celso Augusto Guimarães Santos [c,*]

[a] UFPB – Federal University of Paraíba, Center for Technology, Graduate Program in Civil and Environmental Engineering, Brazil
[b] UFPB – Federal University of Paraíba, Center for Exact and Natural Sciences, Department of Geosciences, Brazil
[c] UFPB – Federal University of Paraíba, Center for Technology, Department of Civil and Environmental Engineering, Brazil

ARTICLE INFO

Article history:
Received 12 January 2019
Received in revised form 10 October 2019
Accepted 10 October 2019

Keywords:
Land cover change
Dynamic modeling
Artificial neural network

ABSTRACT

Accelerated changes in land cover cause changes in environmental dynamics and may cause land degradation. The goals of the present paper were to analyze changes in land cover and to estimate a future scenario for 2035 using an artificial neural network for the Taperoá River basin, located in northeastern Brazil. The classification of land cover was carried out for years t_1 (1990), t_2 (1999) and t_3 (2002), with the latter being used to validate the land cover prediction to obtain an estimate for year t_4 (2035). The land cover classes identified in the basin were (a) water bodies, (b) tree-shrub vegetation, (c) shrub vegetation, (d) herbaceous-shrub vegetation, and (e) herbaceous vegetation. The results of the classifications and of the land cover prediction were analyzed using the kappa coefficient, total operating characteristic (TOC), and area under the curve (AUC). The dynamic modeling of the land cover was based on a multilayer perceptron (MLP) neural network, which presented very good results, with an accuracy = 89.69% after 10,000 iterations, kappa = 0.61 and AUC = 0.67. The results of the land cover change analysis showed a decrease in the tree-shrub class and an increase in the shrub vegetation class between the years analyzed. The scenario predicted for 2035 showed an increase in the herbaceous-shrub vegetation class and a decrease in the area occupied by tree-shrub vegetation.
© 2019 The Authors. Published by Elsevier B.V. This is an open access article under the CC BY-NC-ND license (http://creativecommons.org/licenses/by-nc-nd/4.0/).

1. Introduction

Changes in land cover generated by anthropogenic actions are responsible for changing landscape characteristics and modifying the dynamics of natural processes in river basins (Mendoza et al., 2011) and are of great interest to researchers due to their impact on the local and global environment (Abuelaish and Olmedo, 2016). The main causes of land cover changes vary according to the nature and extent of the area but include deforestation, changing to pasture, agricultural intensification, and overexploitation (Bezak et al., 2015).

Spatial changes in land cover over time also affect the future provision and localization of ecosystem services in the landscape and the fragmentation of green areas (Hoyer and Chang, 2014; Bai et al., 2019). Changes in land cover pose threats

* Corresponding author.
E-mail addresses: lpsjampa@gmail.com (L.P. Silva), anapcxavier@gmail.com (A.P.C. Xavier), richarde@geociencias.ufpb.br (R.M. da Silva), celso@ct.ufpb.br (C.A.G. Santos).

https://doi.org/10.1016/j.gecco.2019.e00811
2351-9894/© 2019 The Authors. Published by Elsevier B.V. This is an open access article under the CC BY-NC-ND license (http://creativecommons.org/licenses/by-nc-nd/4.0/).

to landscapes, for example, by removing characteristic features of the landscape by scale enlargement or deterioration due to lack of management (Schulp et al., 2019).

The risk of these problems is even higher in the semiarid region of Brazil due to the lack of studies regarding the phenological behavior of the vegetation and the recurrence of droughts and rainfall variability, together with the geology of the region and the saline soil types (Silva et al., 2018a). The characteristics of the Caatinga biome make it difficult to produce forecasting maps of the vegetation cover due to the prolonged dry season in the region, which influences the spectral response of the vegetation and, consequently, the estimates of land cover changes (Santos et al., 2017).

Therefore, studying the temporal dynamics and future land cover trends in river basins is extremely important for understanding anthropogenic and environmental processes. It assists in both land and natural resource planning, mainly in river basins located in semiarid regions, which are characterized by traditional forms of vegetation cover marked by extensive grazing, poorly managed traditional agriculture, and inadequate land cover techniques (de Paula Filho et al., 2019).

The use of computational algorithms for the detection and monitoring of land cover changes has been increasing (Zare et al., 2017; Singh et al., 2015; Fan et al., 2008; Islam et al., 2018). These algorithms consider various social, environmental, institutional and economic factors and processes (Keshtkar and Voigt, 2016; Mas et al., 2014; Soares-Filho et al., 2013).

The Markov chain (MC) (Anand et al., 2018), artificial neural network (Azari et al., 2016), cellular automata (Sinha et al., 2015), cellular automata-Markov model (Islam et al., 2018), binary logistic regression (Liu et al., 2017), and similarity-weighted instance-based machine learning algorithm (Mozumder et al., 2016) approaches are some commonly used models for the future prediction and simulation of changes in land cover.

Land-cover change models are applied in various environments (urban and rural) and in various parts of the world. Pacheco and Hewitt (2014) and Megahed et al. (2015) used two methods based on artificial neural networks to model land use and land cover changes in urban environments in Egypt. Other examples are the studies of Lira et al. (2012) in São Paulo and Vega et al. (2017) in Spain, who analyzed changes in rural areas, taking into account both pessimistic and optimistic scenarios (with the regeneration of vegetation cover).

However, in Brazil, the use of prediction algorithms for land cover is still rare (Barros et al., 2018; Santini et al., 2010) and has focused on humid environments (Couto Júnior et al., 2019; Monteiro Junior et al., 2018; dos Santos et al., 2018; Lima et al., 2012) because the cloud cover is a constraint for obtaining optical orbital data (Sano et al., 2007). Thus, land use and land cover prediction is more common for small and mainly urban areas. For example, one can cite the study of de Almeida et al. (2005) that modeled land use and land cover changes through geographical information systems, remote sensing imagery and Bayesian probabilistic methods using a simulation model named DINAMICA. Almeida et al. (2008) applied artificial neural networks and a cellular automaton simulation model based on stochastic transition rules to estimate changes in land use and land cover in the urban area of Piracicaba, located in southeastern Brazil, to analyze the influence of growth on landscape transformation. Xavier and Silva (2018) estimated land use and occupation in the Tapacurá River basin, located in northeastern Brazil. The results indicated that the methodology is robust, presenting satisfactory results for the comparison between the reference and predicted maps for the study region.

These applications present different climatic and vegetative aspects from those of the Taperoá River basin, located in the semiarid region of Brazil, which is characterized by prolonged drought periods, high rates of evapotranspiration and the presence of the Caatinga biome (quite susceptible to deforestation and climate changes). In addition, the Taperoá River is the largest tributary of the Paraíba River, and the two together drain water to the second largest reservoir in Paraíba, the Epitácio Pessoa. This reservoir is responsible for the human and industrial supply of Campina Grande city and surrounding areas and is considered highly important in the context of the water resources of the Paraíba state.

Thus, due to the relevance of the Taperoá River basin to the development and quality of life of the region and the unique characteristics of environmental degradation, the scarcity of studies on the future prediction of land cover and the increasing changes in land cover in the semiarid region of Brazil, the ability of this work to issue warning and provide support for decision making is an important contribution. Therefore, this study aims to predict the possible land cover pattern in the Taperoá River basin for the year 2035 using an algorithm based on artificial neural networks. This environment is marked by the intense interaction of the typical vegetation of the Caatinga biome with the soil and atmosphere and by long periods of drought, which most often immediately influence the dynamics of the region's land cover.

2. Materials and methods

2.1. Location and description of the study area

The Taperoá River basin comprises an intermittent drainage network located in the semiarid region of the state of Paraiba, located in northeastern Brazil. This basin has an area of approximately 5660 km^2 and lies between the geographic coordinates 6°40′0″ and 7°40′0″ south latitude and 36°00′0″ and 37°20′0″ west longitude (Fig. 1).

According to the Köeppen climate classification, the climate in the Taperoá River basin is type BSh (semiarid – hot and dry) and is characterized by summer rains and elevated temperatures higher than 27 °C (de Medeiros et al., 2018). The mean annual rainfall in the basin is approximately 500 mm, and the area is characterized by poorly distributed rains, long drought periods during the year (from 8 to 9 months), a relative air humidity of 78%, a high number of hours of sun exposure, a high evapotranspiration rate, and a high water deficit during a large portion of the year (Silva et al., 2018b).

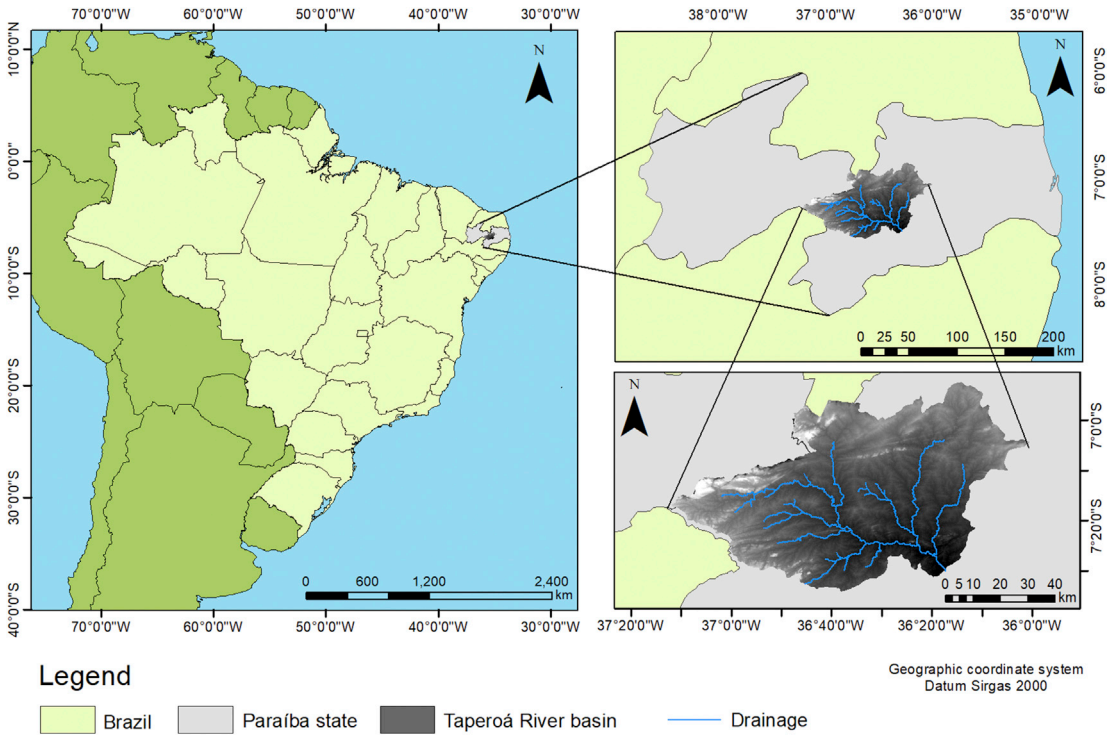

Fig. 1. Geographical location of the Taperoá River basin in Brazil.

The vegetation that makes up the Taperoá River basin, as well as most of the Brazilian semiarid region, is the Caatinga, a biome dominated by xerophytic deciduous species, with a strong presence of thorny plants and good adaptation to drought. The size of this type of vegetation is influenced by soils and relief and therefore varies according to the diversity of landscapes that cover the semiarid region. The topographic variability and the distribution of soil types influence the variation in vegetation size and species (Souza et al., 2009).

The predominant soils in the Taperoá River basin are Litholic Neosols (35.5%), Luvisols (25.5%), Planosols (16.3%), Regolithic Neosols (14%), Flubic Neosols (5%), Vertisols (2.3%), Cambisols (1.3%) and Oxisols (0.1%). Litholic Neosols occupy the largest area of the basin and are constituted in large part by fragments of rock larger than 2 mm, presenting direct contact between horizons A and C; in some cases, a poorly developed B horizon may be present (EMBRAPA, 2006).

2.2. Selection and processing of the satellite images

For this study, three satellite images were selected: t_1 (1990), t_2 (1999) and t_3 (2002), as showed Table 1. Land cover mapping of the Taperoá River basin was performed based on Landsat satellite images with a spatial resolution of 30 m, obtained from the United States Geological Survey platform (Geological Survey, 2018). These images were chosen because they do not contain clouds over the basin area; clouds are a great obstacle for the interpretation and classification of satellite images of the Brazilian semiarid region. Thus, images with a maximum cloud cover of 20% were chosen.

Image processing (georeferencing and classification) was carried out in a geographic information system (GIS) environment. For the interpretation and analysis of the satellite images, the following land cover classes were defined: (a) water bodies, (b) tree-shrub vegetation, (c) shrub vegetation, (d) herbaceous-shrub vegetation, and (e) herbaceous vegetation. Table 2 shows descriptions of the vegetation cover classes identified for the Taperoá River basin. The images were classified by the supervised classification method, and the classifier type was the Maxver, which takes into account the weighting of the distances between the means of the digital stages of the classes and statistical parameters (Churches et al., 2014).

Table 1
Characteristics of the images used in the classification of the land cover in the Taperoá River basin.

Date	Satellite	Sensor	Orbit	Point	Bands	Resolution
June 18, 1990	Landsat 5	TM	215	065	5-4-3 (RGB)	30 m
August 04, 1999	Landsat 5	TM	215	065	5-4-3 (RGB)	30 m
July 07, 2002	Landsat 7	TM	215	065	5-4-3 (RGB)	30 m

Table 2
Description of the land cover classes used in the present study.

Classes	Description
Water bodies	Natural and artificial lakes
Tree-shrub vegetation	Predominant trees surrounded by shrubs
Shrub vegetation	Predominant shrubs
Herbaceous-shrub vegetation	Predominant shrubs, weeds and grasses
Herbaceous vegetation	Predominant weeds and grasses or little vegetation

The image classification performance was evaluated using the kappa coefficient of agreement (Landis and Koch, 1977). The kappa coefficient can be obtained with the following equation (Cohen, 1960):

$$I = \frac{n\sum_{i=1}^{c} x_{ii} - \sum_{i=1}^{c} x_{i+}x_{+i}}{n^2 - \sum_{i=1}^{c} x_{i+}x_{+i}} \quad (1)$$

where I = kappa coefficient; x_{ii} = value in row i and column i, x_{i+} = sum of row i, x_{+i} = sum of column i of the matrix, n = total number of observations, and c = total number of classes. The kappa coefficient classification adopted in this study to evaluate the quality of the classified maps was based on Landis and Koch (1977), who defined the degree of agreement as (a) poor: < 0, (b) slight: 0–0.2, (c) fair: 0.21–0.4, (d) moderate: 0.41–0.6, (e) substantial: 0.61–0.8, and (f) almost perfect: 0.81–1.0.

For each image, the kappa coefficient was calculated for a sample area with dimensions of 274 rows × 420 columns, totaling an area of 103.54 km^2 (Fig. 2), as described by Santana et al. (2014). Subsequently, a mesh of 60 known sample pixels was created in each image, and a confusion matrix of the samples and the classified points of the image was generated. Next, the agreement between the pairs was calculated based on that confusion matrix, and a matrix of the transition probability of land cover classified for t_2 (1999) and t_3 (2002) in the Taperoá River basin was obtained.

2.3. Prediction of land cover

This study used an artificial neural network model named the multilayer perceptron (MLP) (Haykin, 2001). The MLP network performs orbital image classification by means of an artificial neural network classifier using the back propagation algorithm. The Land Change Modeler (LCM) module of IDRISI TerrSet software was used to run the MLP, since this modeling tool has shown satisfactory results in studies of this nature for the northeastern Brazil and several other parts of the world (Mishra et al., 2014; Xavier and Silva, 2018; Nasiri et al., 2018). The MLP allows the testing and definition of several transitions and consequently a better analysis of the transition potential of soil cover classes.

To run the MLP, the variables controlling the land cover changes are input as independent variables, and the land cover images are input as dependent variables. The prediction model was applied to detect if the predicted land cover map yielded satisfactory results compared to the real world map (observed).

The classified images from 1990, 1999 and 2002 along with the transition probabilities predicted in the MLP model are used to simulate the scenario in 2035. The change analysis tab of LCM determines the tendency of change and the persistently changed pixels of the different land cover classes. It also produces a change map based on the previous (1990) and later (1999) images.

In this work, the dynamic modeling consisted of three main steps: (a) prediction of transition potential, (b) simulation (including evaluation of the artificial neural network and application of the MC), and (c) validation. Fig. 3 presents a flowchart of the methodology used in this study.

For the transition potential prediction step, the main land cover changes in the basin between t_1 (1990) and t_2 (1999) were analyzed. These analyses are necessary for the definition of the transition classes. Subsequently, the transition classes were

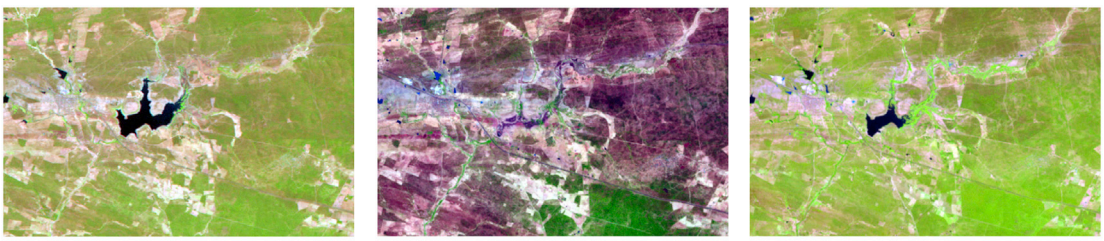

Fig. 2. Sample area for the years (a) 1990, (b) 1999 and (c) 2002.

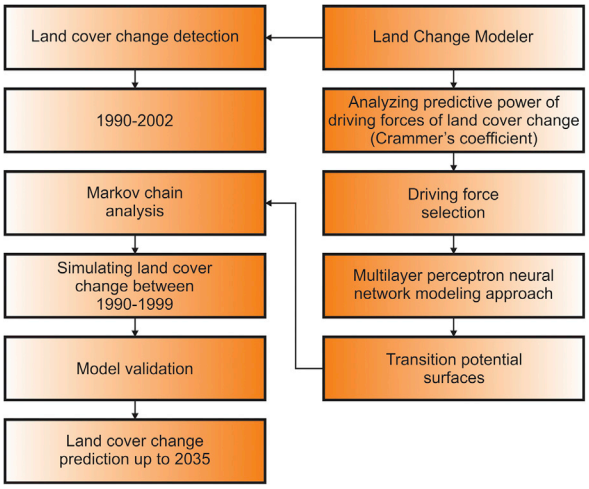

Fig. 3. Methodology flowchart (adapted from Nasiri et al., 2018).

defined, and explanatory variables were selected using the Cramer test. In this study, variables presenting Cramer values > 0.15 were considered in the modeling of land cover, as recommended by Hamdy et al. (2017). The variables altitude, slope, economic indicators, distance of roads, distance from urban centers, distance from water courses and transition distance of classes are important test in the modeling of changes in land use and land cover (Han et al., 2015; Islam et al., 2018). Therefore, based on the changes of the land cover in the basin and the literature, the following explanatory variables were selected for testing: (a) altimetry, (b) declivity, (c) roads and highways, (d) water courses, (e) distance from water courses, (f) distance from roads and highways, (g) distance from transition between arboreal vegetation and tree-shrub vegetation, (h) distance from transition between herbaceous vegetation and herbaceous-shrub vegetation, (i) distance from changes between 1990 and 1999, and (j) distance from the probability of change between 1990 and 1999.

The Cramer test uses values between 0 and 1, such that the closer the value is to 1, the larger is the association between the explanatory variable and the defined transition classes. The Cramer test is a nonparametric statistical analysis, i.e., it is applicable regardless of the variable distribution. This analysis is used to measure the strength of the association between variables (Liebertrau, 1983; Islam et al., 2018; Valdivieso and Sendra, 2010). This test is obtained with Eq. (2):

$$V = \sqrt{\frac{\chi^2}{n(q-1)}} \tag{2}$$

where χ^2 = chi-square coefficient:

$$\chi^2 = \frac{(O-E)^2}{2} \tag{3}$$

and V = Cramer's index, n = sample size, q = smallest value in the rows and columns of the land cover image, O = observed frequency for a category, and E = expected frequency in the corresponding category.

2.3.1. Evaluation of artificial neural network and application of Markov chain

When the transition classes were defined, the artificial neural network was executed. The method provides an accuracy that depends on the iteration between the explanatory variables and the considered transitions. Thus, several tests were performed to obtain an accuracy greater than or equal to 80%, according to recommendations of Sampaio (2014) and Islam et al. (2018) for the prediction of land cover.

For this study, the standard configuration was used (sample of 50% of the altered pixels were used for MLP training, and the remaining 50% were retained for validation), as recommended by Mishra et al. (2014) and Eastman (2016), with iteration numbers equal to 10,000, since the error curve was observed to decrease and become stable using this number of iterations.

With an MLP accuracy greater than or equal to 80%, the learning algorithm satisfactorily simulates the transition potential of soil cover classes. After achieving such precision, the time t_3 (2002) was specified, and MC was used to obtain the transition probability matrix from t_2 (1999) for t_3 (2002). The MC plots stochastic processes using the following equation:

$$\prod(t+1) = p^n \times \prod(t) \tag{4}$$

where $\Pi(t)$ = system state at time t; $\Pi(t+1)$ = system state after interval $(t+1)$, and p^n represents the possible states demonstrated through the transition possibility matrix.

2.3.1.1. Validation of land cover prediction. In this study, the total operating characteristics (TOC) was used, as well as the error maps to assess the goodness-of-fit of land cover prediction map ($t_4 = 2035$), as recommended by Pontius and Si (2014). The total operating characteristic (TOC) method (Pontius and Si, 2014) was used to evaluate the performance of the probability of changing the land cover produced by the trained MLP. The TOC considers multiple thresholds and, therefore, generates multiple contingency tables. It is helpful to have a method to reveal the information of the entire contingency table for all thresholds efficiently in one graphical plot (Pontius and Si, 2014). This method is frequently used in studies of vegetation cover changes, urbanization and weather forecasting (Du et al., 2015; Ahmadlou et al., 2016; Chen et al., 2019).

In addition, the area under the curve (AUC) obtained by the TOC method can be used to evaluate the simulation accuracy. Such an AUC metric is used frequently to summarize the strength of the overall diagnostic ability. An AUC greater than the baseline value of 0.5 indicates that the quality of the modeling results is satisfactory, and a value of 1 corresponds to a perfect fit (Chen et al., 2019; Islam et al., 2018). After successful validation, the simulation was used to predict the land cover of the Taperoá River basin for the year 2035.

3. Results and discussion

3.1. Changes in land cover in the Taperoá River basin from 1990 to 2002

Fig. 4a–c show the three classified land cover images for the analyzed years, and Fig. 4d presents the prediction of the vegetation cover for 2002, as estimated by MLP and MC. The land cover classifications in 1990, 1999 and 2002 showed good agreement between the classified map of each year and the mesh of pixels of each year used to calculate the kappa coefficient (kappa equal to 0.78, 0.71 and 0.72, respectively); according to Landis and Koch (1977), these values represent good results.

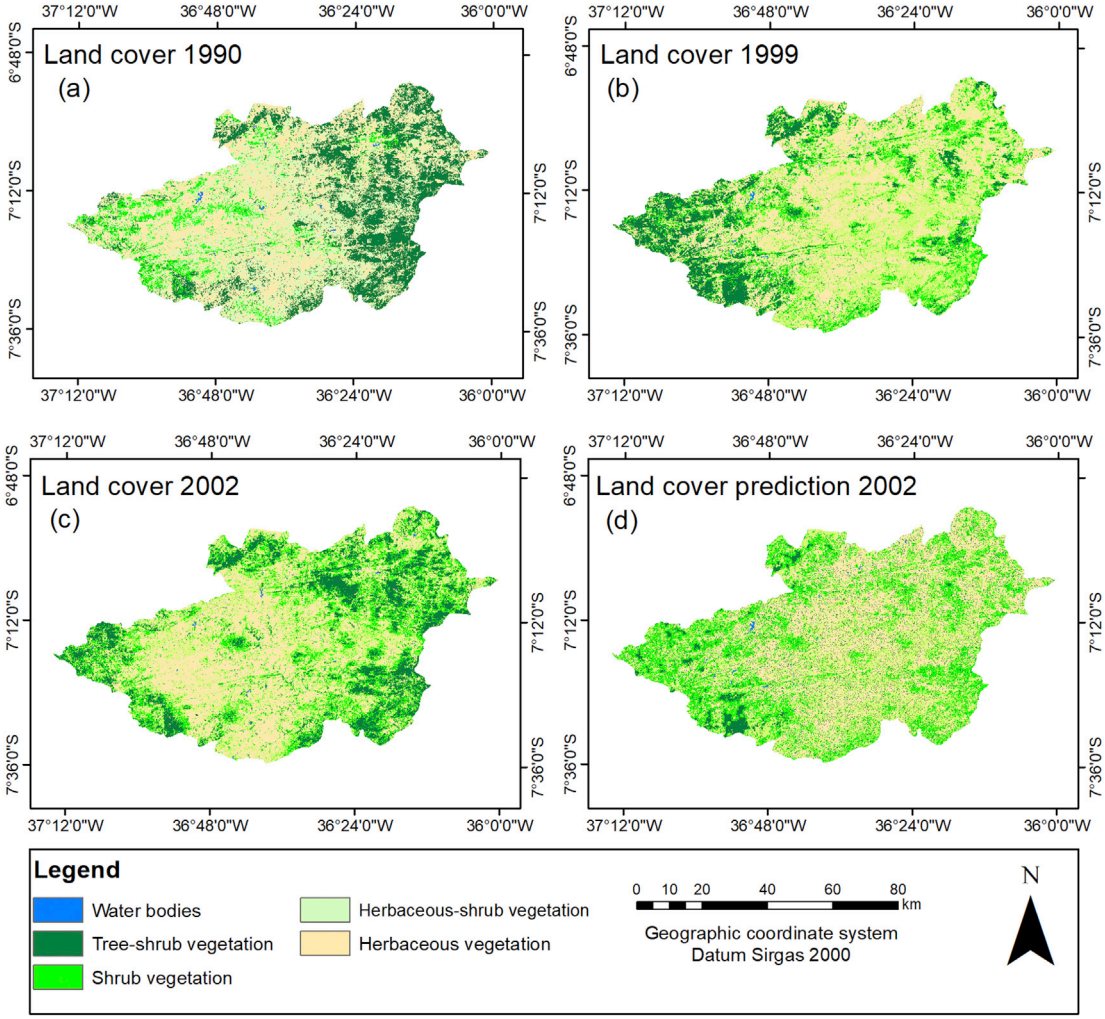

Fig. 4. Land cover maps for the Taperoá River basin for (a) 1990, (b) 1999, and (c) 2002 and (d) estimated land cover map for 2002.

Table 3
Land cover in the Taperoá River basin in 1990, 1999 and 2002.

Classes	1990	1999	2002	Change 1990–2002 (%)
	Area in km^2 (%)	Area in km^2 (%)	Area in km^2 (%)	
Water bodies	14.86 (0.26)	16.5 (0.29)	11.07 (0.2)	−25.50
Tree-shrub vegetation	571.69 (10.08)	829.61 (14.63)	1015.07 (17.9)	77.56
Shrub vegetation	1408.95 (24.85)	1378.22 (24.31)	1577.45 (27.82)	11.96
Herbaceous-shrub vegetation	2187.68 (38.59)	1490.04 (26.28)	1350.72 (23.22)	−38.26
Herbaceous vegetation	1486.35 (26.22)	1953.09 (34.45)	1713.16 (30.22)	15.26

Table 4
Results for the Cramer's V test for the explanatory variables tested in the land cover modeling for the Taperoá River basin.

Explanatory variable	Cramer's V
Distance from transition from tree vegetation to tree-shrub vegetation	0.27
Distance from transition from herbaceous vegetation to herbaceous-shrub vegetation	0.20
Distance from changes between 1990 and 1999	0.81
Distance from probability of changes between 1990 and 1999	0.35
Altimetry	0.08
Declivity	0.04
Roads and highways	0.07
Water courses	0.03
Distance to water courses	0.09
Distance to roads and highways	0.04

For 1990, a predominance of the tree-shrub and herbaceous-shrub vegetation classes was observed in the eastern region of the basin, while in the western region, there is a larger predominance of the herbaceous and shrub vegetation classes. Based on the landscape metrics, the herbaceous-shrub vegetation class had the largest occupied area (2187.68 km^2), corresponding to 38.59% of the area of the Taperoá River basin. The water body class was the smallest occupied area (14.86 km^2).

The results showed that the herbaceous vegetation class was the most representative (34.45%) in the year t_2 (1999). In the eastern region of the basin, there was a change from the tree-shrub vegetation class to the shrub class. When compared to the map for t_1 (1990), the same type of change was identified for the western region of the basin; however, the transition was from the shrub to the tree-shrub vegetation class.

For the year t_3 (2002), the herbaceous vegetation (30.22%) and shrub vegetation (27.82%) classes showed the largest occupied areas. In the eastern region of the basin, predominance of the shrub vegetation class and decreases in herbaceous and herbaceous-shrub vegetation classes were observed. On the western side, there was a loss in the tree-shrub vegetation class and an increase in the shrub vegetation class compared to the map for 1999.

An increase in the herbaceous vegetation class was observed in 1999 and 2002. This result is entirely related to the observed rainfall reduction for the period 1999 to 2012 in the Taperoá River basin (AESA, 2013; Santos et al., 2019) because the vegetation of the semiarid region is slightly influenced by the climatic conditions. During dry periods, the foliage of the plants is reduced, which influences the size and the spectral response of the vegetation.

The obtained land cover maps show that the class of water bodies showed a reduction in area occupied in 2002. The tree-shrub vegetation class showed an increase in all three years. The shrub class decreased from the first period to the second period and increased from the second period to the third period. The herbaceous-shrub vegetation class presented consecutive decreases in all three years. Herbaceous vegetation increased from the first to the second and showed a small decrease in the third period but remained the class occupying the largest area in 2002. Table 3 presents the areas for each thematic class identified in the Taperoá River basin for the three studied years and the percentage change in area from 1990 to 2002.

The shrub vegetation class presented satisfactory spatial location hits in the comparison between the land cover classifications for 2002 (Fig. 4c) and the simulation (Fig. 4d). In contrast, for the tree-shrub vegetation class, the modeling presented good results only for the southwest region and for some areas in the north region of the basin, while in the classified map, this class was also found in the east and northeast regions of the basin.

In addition to climatic factors, the growing demand for food promoted changes in land cover and increased rates of deforestation in the Brazilian semiarid region. For the period from 1990 to 2010, the areas occupied by herbaceous vegetation in the Brazilian semiarid region grew; as a consequence of this scenario, these areas may become more susceptible to the desertification process (Menezes et al., 2012; Sousa et al., 2012; Beuchle et al., 2015).

3.2. Modeling of the estimated land cover

Table 4 shows the explanatory variables obtained from the Cramer's V test for the 2002 land cover modeling for the Taperoá River basin. The explanatory variables considered in the modeling were (a) distance from the transition from tree

vegetation to tree-shrub vegetation, (b) distance from the transition from herbaceous vegetation to herbaceous-shrub vegetation, (c) distance from changes between 1990 and 1999, and (d) distance from the change probability between 1990 and 1999, since these explanatory variables had Cramer values greater than 0.15.

The variable “distance from changes between 1990 and 1999” was the most significant according to the Cramer's V test. This result indicated that the changes that occurred between 1990 and 1999 were significant for the modeling and that there is a higher possibility of continued change behavior in the land cover for the future scenario in areas close to those that have already undergone changes in land cover. However, the lowest result was obtained for the “roads and highways” variable, which indicated that this variable had low significance in the land cover prediction for the basin.

For the dynamic modeling of land cover, the best training result based on the MLP algorithm, obtained from the iteration of the explanatory variables with the transitions of interest, had an accuracy rate equal to 89.69% after 10,000 iterations.

Table 5 presents the land cover transition probability matrix of t_2 (1999) for t_3 (2002) obtained by MC. The results of the diagonal represent the percentages of persistence, while the other results correspond to the percentages of change from one land cover category to another. The herbaceous vegetation, water bodies and herbaceous-shrub vegetation classes had a probability of persistence greater than 50%. However, the highest probability of change was from the shrub vegetation class to the tree-shrub vegetation, at 74%.

Table 6 compares the classified image for 2002 and the estimated images for 2002 obtained by dynamic modeling. The results show that the area occupied by water bodies, shrub vegetation and herbaceous-shrub vegetation classes were overestimated. Conversely, the herbaceous vegetation and tree-shrub vegetation classes showed lower occupied areas than in the classified map. Despite this difference in the occupied area between the classified and estimated maps, the results obtained showed good agreement between the classified and estimated images, with kappa = 0.61, indicating that the land cover model provided a satisfactory prediction for the study area, according to the classification proposed by Landis and Koch (1977). Fig. 5 shows the changes in percentage area for each of the classes analyzed in the observed and predicted images for 2002.

Table 5
Matrix of the transition probability of land cover categories for t_2 (1999) and t_3 (2002) in the Taperoá River basin.

1999	2002				
	Water bodies	Tree-shrub vegetation	Shrub vegetation	Herbaceous-shrub vegetation	Herbaceous vegetation
Water bodies	0.5741	0.0000	0.1749	0.1377	0.1132
Tree-shrub vegetation	0.0016	0.1370	0.5630	0.2851	0.0000
Shrub vegetation	0.0000	0.7420	0.2081	0.0499	0.0000
Herbaceous-shrub vegetation	0.0008	0.0000	0.1942	0.5495	0.2555
Herbaceous vegetation	0.0020	0.0000	0.0771	0.1259	0.7949

Table 6
Comparison between the classified and estimated images for 2002.

Land cover class	Area (km^2)		Error (%)
	Classified map	Prediction	
	2002	2002	
Water bodies	11.07	14.92	34.78
Tree-shrub vegetation	1015.07	622.23	38.70
Shrub vegetation	1577.45	1678.62	6.41
Herbaceous-shrub vegetation	1350.72	1807.15	33.79
Herbaceous vegetation	1713.16	1544.54	9.84

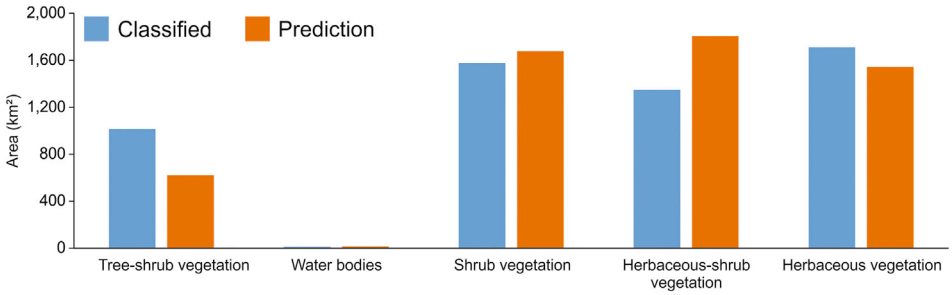

Fig. 5. Classified and simulated (predicted) land cover for the analyzed classes for 2002.

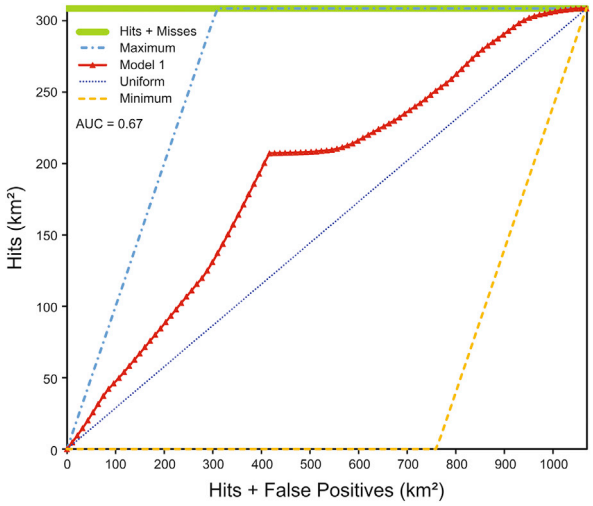

Fig. 6. AUC and TOC curve for the evaluation of land cover prediction in 2002 based on an artificial neural network in the Taperoá River basin.

Table 7
Matrix of omission and commission errors.

Land cover	Water bodies	Tree-shrub vegetation	Shrub vegetation	Herbaceous-shrub vegetation	Herbaceous vegetation	Omission (%)	Commission (%)
Water bodies	11,220	4722	2846	1856	3748	54,00%	44,22%
Tree-shrub vegetation	1170	546,027	204,711	151,734	167,851	49,04%	63,79%
Shrub vegetation	2413	667,308	2,209,403	327,589	196,546	35,08%	32,86%
Herbaceous-shrub vegetation	2702	252,740	652,099	1,907,982	520,705	42,81%	32,56%
Herbaceous vegetation	2610	37,183	221,787	439,922	3,339,585	17,36%	21,02%

Fig. 6 shows the TOC result used to evaluate the performance of the probability of land cover change produced by the trained MLP. TOC curves were used to assess the predictive ability of the transition suitability maps, which were evaluated against the corresponding reference land cover maps (between 1999 and 2002). The obtained AUC was 0.67, which is greater than the random baseline AUC of 0.5, indicating satisfactory prediction of the land cover by MLP. In general, the TOC curve showed average accuracy at most limits, with a curve above the random line and greater precision at low thresholds at the lower left of the curve.

The maximum and minimum boundaries form a parallelogram that contains the mathematically possible space where the TOC curve appears. A diagonal dotted line joins the lower left corner to the upper right corner within the TOC parallelogram. This dotted line shows the statistically expected results for a hypothetical index variable that has values assigned at random (Pontius and Si, 2014).

Table 7 shows the confusion matrix with omission and commission errors obtained by comparing the classification and prediction of land cover in the Taperoá River basin in 2002. The class that showed the largest omission error was water bodies (54%), and as for commission, the tree-shrub vegetation was the class with the largest error (63.79%); however, the herbaceous vegetation class showed lower omission and commission errors and consequently better prediction of land cover.

Fig. 7 presents the spatial validation of the prediction of land cover in the Taperoá River basin in 2002. The region with the most prediction hits was the central portion of the basin occupied mainly by the herbaceous vegetation class. The largest prediction errors (misses) were found in the northeastern, eastern and southeastern regions of the basin. For the western region of the basin, the prediction resulted in class changes; however, such areas did not show significant changes (false alarms).

Low agreements with actual changes in land cover may be related to non-gradual changes observed in 1990 and 1999; possibly, climate features may have strongly affected the spectral response of existing vegetation cover in the basin. Climate characteristics and the lack of satellite images without clouds are factors that may affect the future prediction of changes in land cover, especially in semiarid regions such as the Taperoá River basin.

3.2.1. Land cover prediction for 2035

The land cover prediction for 2035 showed a decreasing trend for the tree-shrub vegetation areas, mainly in the northeastern region of the basin (Fig. 8), along with fragmentation of the herbaceous vegetation (central region) and an increase in

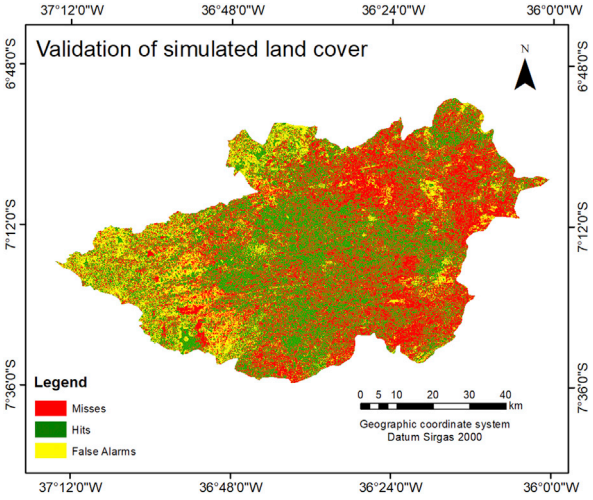

Fig. 7. Spatial validation of simulated land cover for the Taperoá River basin in 2002.

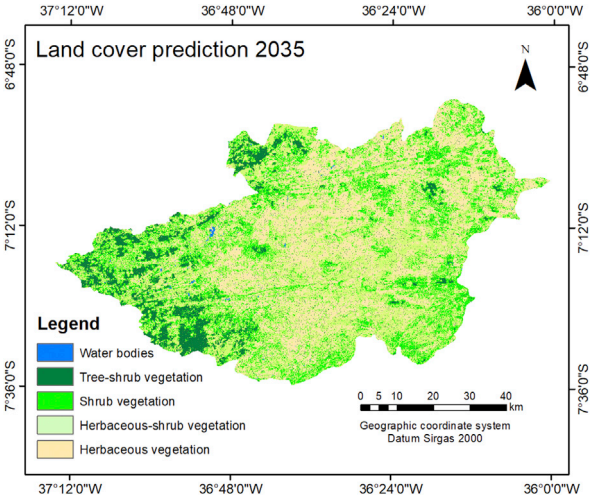

Fig. 8. Land cover prediction for 2035 for the Taperoá River basin.

Table 8
Land cover of the Taperoá River basin for year t_4 (2035).

Classes	Area (km^2)	Area (%)
Water bodies	16.00	0.28
Tree-shrub vegetation	534.80	9.44
Shrub vegetation	1552.52	27.39
Herbaceous-shrub vegetation	2142.62	37.81
Herbaceous vegetation	1421.53	25.08
Area of the basin	5667.46	100.00

the herbaceous-shrub vegetation to the east of the basin. The modeling showed that the disposition of the herbaceous-shrub, shrub and herbaceous vegetation classes was the most significant, with occupied area percentages of 37.81%, 27.39% and 25.08%, respectively (Table 8).

In the eastern region of the basin, an increase in the area occupied by the herbaceous vegetation class and a change from the tree-shrub vegetation class to the shrub vegetation class were observed for t_4 (2035). However, in the western region, the herbaceous vegetation class decreased and was replaced by the herbaceous-shrub and shrub vegetation classes. In the

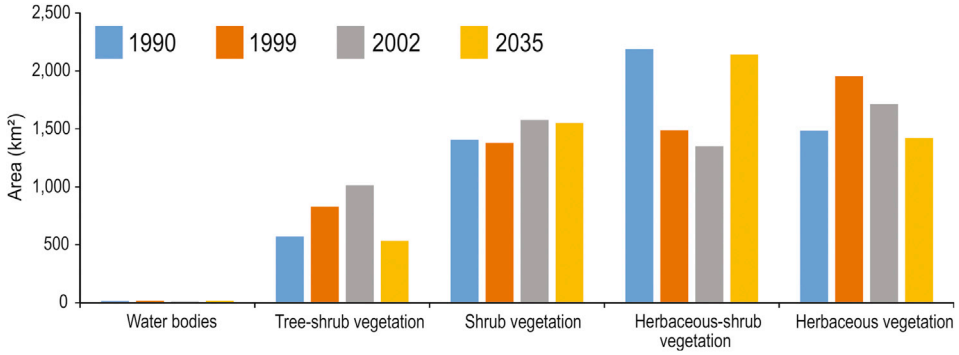

Fig. 9. Areas occupied (km^2) by the land cover classes in the Taperoá River basin in 1990, 1999, 2002 and 2035.

southwest area of the basin, the modeling showed an increase in the tree-shrub vegetation class and a decrease in the shrub vegetation.

Fig. 9 shows the behavior of the land cover classes in 1990, 1999, and 2002 and in the predicted scenario for 2035. The water body class did not show significant changes across the four years; however, the areas occupied by tree-shrub vegetation decreased for 2035, as well as in 1999 (approximately 500 km^2). The shrub vegetation class in 2035 presented basically the same occupied area as in 2002. In contrast, the herbaceous-shrub vegetation and herbaceous vegetation classes occupied area values similar to those in 1990.

In general, regarding the behavior of the land cover in the Taperoá River basin in 2035, the model predicted occupied areas similar to those in 1990 but nevertheless demonstrated a possible reduction in the arboreal-shrub class. This result shows the prediction of a year that is probably drier than 2002. The results of this research could help in the formulation of public policies designed to conserve environmental resources in the Taperoá River basin and, consequently, minimize the risks of degradation of the water resources, a precious resource in the context of the Brazilian semiarid region. Based on the identification of areas most vulnerable to future land cover changes, some soil conservation practices could be adopted to minimize such risks of degradation. For example, policies of payment for environmental services (PES) could be implemented in the basin, as practiced in several regions of the world, e.g. China (Chen et al., 2014), Minas Gerais state in Brazil (Zolin, 2010), and United States (Postel and Thompson, 2005). The present results could also serve as a basis for further studies on the prediction of hydrological, climatic and sedimentological factors to which the region may be subject and that would influence the entire environmental dynamics of the basin.

For future works on land cover dynamics in the Taperoá River basin, it is suggested that high-spatial-resolution satellite images could be used to facilitate not only the identification of vegetation cover classes but also the identification of land use cover in the study region and to include other explanatory variables that may affect these dynamics, such as future population growth, the construction of ventures with great impact on the landscape (if any), and aspects of changes in the rainfall regime to which the area may be subject, among others. It is worth noting that for this study, these variables were not considered because the objective was to predict the land cover scenario based mainly on the changes observed between 1990 and 2002, not taking into account future climatic and population aspects.

4. Conclusions

This study identified the land cover changes that occurred in the Taperoá River basin between the years t_1 (1990), t_2 (1999) and t_3 (2002). The main land cover change for 2002 compared to 1990 was the decrease in the tree-shrub vegetation class and its replacement by the shrub vegetation class; this behavior was mostly observed in the eastern region of the basin. The land cover dynamic modeling based on the MLP neural network showed satisfactory results for the Taperoá River basin, with an accuracy of 89.69% after 10,000 iterations and a kappa coefficient of 0.61, classified according to Landis and Koch (1977) as good quality and AUC curve of 0.67. The predicted scenario for t_4 (2035) showed a considerable increase in the herbaceous-shrub vegetation class, which was the most common class, representing approximately 38% of the area, and a decrease in the area occupied by tree-shrub vegetation compared to that in 2002.

Declaration of competing interest

The authors declare no conflict of interest in the manuscript “Modeling land cover change based on an artificial neural network for a semiarid river basin in northeastern Brazil”, which we would like to submit for publication as an Original Article in the Global Ecology & Conservation.

Acknowledgments

The financial support provided by the National Council for Scientific and Technological Development, Brazil (Grant No. 304213/2017-9 and 304540/2017-0), is gratefully acknowledged. This study was also financed in part by the Coordenação de Aperfeiçoamento de Pessoal de Nível Superior – Brazil (CAPES) – Finance Code 001, and Federal University of Paraíba.

Appendix A. Supplementary data

Supplementary data to this article can be found online at https://doi.org/10.1016/j.gecco.2019.e00811.

References

Abuelaish, B., Olmedo, M.T.C., 2016. Scenario of land use and land cover change in the Gaza Strip using remote sensing and GIS models. Arabian J. Geosci. 9 (4), 274. https://doi.org/10.1007/s12517-015-2292-7.

AESA – Agência Executiva de Gestão das Águas, 2013. Portal GEOAESA. http://siegrh.aesa.pb.gov.br:8080/aesa-sig/. (Accessed 15 May 2013).

Ahmadlou, M., Delavar, M.R., Tayyebi, A., 2016. Comparing ANN and CART to model multiple land use changes: a case study of Sari and Ghaem-Shahr cities in Iran. J. Geomatics Sci. Technol. 6 (1), 292–303.

Almeida, C.M., Gleriani, J.M., Castejon, E.F., Soares-Filho, B.S., 2008. Using neural networks and cellular automata for modelling intra-urban land-use dynamics. Int. J. Geogr. Inf. Sci. 22 (9), 943–963. https://doi.org/10.1080/13658810701731168.

Anand, J., Gosain, A.K., Khosa, R., 2018. Prediction of land use changes based on Land Change Modeler and attribution of changes in the water balance of Ganga basin to land use change using the SWAT model. Sci. Total Environ. 644, 503–519. https://doi.org/10.1016/j.scitotenv.2018.07.017.

Azari, M., Tayyebi, A., Helbich, M., Reveshty, M.A., 2016. Integrating cellular automata, artificial neural network, and fuzzy set theory to simulate threatened orchards: application to Maragheh Iran. GIScience Remote Sens. 53 (2), 183–205. https://doi.org/10.1080/15481603.2015.1137111.

Bai, Y., Ochuodho, T.O., Yang, J., 2019. Impact of land use and climate change on water-related ecosystem services in Kentucky, USA. Ecol. Indicat. 102, 51–64. https://doi.org/10.1016/j.ecolind.2019.01.079.

Barros, K.O., Ribeiro, C.A.A.S., Marcatti, G.E., Lorenzon, A.S., de Castro, N.L.M., Domingues, G.F., de Carvalho, J.R., dos Santos, A.R., 2018. Markov chains and cellular automata to predict environments subject to desertification. J. Environ. Manag. 225 (1), 160–167. https://doi.org/10.1016/j.jenvman.2018.07.064.

Beuchle, R., Grecchi, R.C., Shimabukuro, Y.E., Seliger, R., Eva, H.D., Sano, E., Achard, F., 2015. Land cover changes in the Brazilian Cerrado and Caatinga biomes from 1990 to 2010 based on a systematic remote sensing sampling approach. Appl. Geogr. 58, 116–127. https://doi.org/10.1016/j.apgeog.2015.01.017.

Bezak, N., Rusjan, S., Petan, S., Sodnik, J., Mikos, M., 2015. Estimation of soil loss by the WATEM/SEDEM model using an automatic parameter estimation procedure. Environ. Earth Sci. 74, 5245–5261. https://doi.org/10.1007/s12665-015-4534-0.

Chen, X., Viña, A., Shortridge, A., An, L., Liu, J., 2014. Assessing the effectiveness of payments for ecosystem services: an agent-based modeling approach. Ecol. Soc. 19 (1), 7.

Chen, Y., Li, X., Liu, X., Zhang, W., Huang, M., 2019. Tele-connecting China's future urban growth to impacts on ecosystem services under the shared socioeconomic pathways. Sci. Total Environ. 652, 765–779. https://doi.org/10.1016/j.scitotenv.2018.10.283.

Churches, C.E., Wampler, P.J., Sun, W., Smith, A.J., 2014. Evaluation of forest cover estimates for Haiti using supervised classification of Landsat data. Int. J. Appl. Earth Obs. Geoinf. 30 (2), 203–216. https://doi.org/10.1016/j.jag.2014.01.020.

Cohen, J., 1960. A coefficient of agreement for nominal scales. Educ. Psychol. Meas. 20 (1), 37–46. https://doi.org/10.1177/001316446002000104.

Couto Júnior, A.A., da Conceição, F.T., Fernandes, A.M., Spatti Junior, E.P., Lupinacci, C.M., Moruzzi, R.B., 2019. Land use changes associated with the expansion of sugar cane crops and their influences on soil removal in a tropical watershed in São Paulo State (Brazil). Catena 172, 313–323. https://doi.org/10.1016/j.catena.2018.09.001.

de Almeida, C.M., Monteiro, A.M.V., Câmara, G., Soares-Filho, B.S., Cerqueira, G.S., Pennachin, C.L., Batty, M., 2005. GIS and remote sensing as tools for the simulation of urban land-use change. Int. J. Remote Sens. 26 (4), 759–774. https://doi.org/10.1080/01431160512331316865.

de Medeiros, I.C., de Costa Silva, J.F.C.B., Silva, R.M., Santos, C.A.G., 2018. Run-off-erosion modelling and water balance in the Epitácio pessoa dam River basin, Paraiba state in Brazil. Int. J. Environ. Sci. Technol. 15 (1), 1–14. https://doi.org/10.1007/s13762-018-1940-3.

de Paula Filho, F.J., Sampaio, A.D.S., Menezes, J.M.C., Da Costa, C.T.F., Santiago, M.O., 2019. Land uses, Nitrogen and Phosphorus estimated fluxes in a Brazilian semiarid watershed. J. Arid Environ. 163, 41–49. https://doi.org/10.1016/j.jaridenv.2019.01.001.

dos Santos, U.S., De Medeiros, E.V., Duda, G.P., Marques, M.C., de Souza, E.S., Brossard, M., Hammecker, C., 2018. Land use changes the soil carbon stocks, microbial biomass and fatty acid methyl ester (FAME) in Brazilian semiarid area. Arch. Agron Soil Sci. https://doi.org/10.1080/03650340.2018.1523544.

Du, S., Rompaey, A.V., Shi, P., Wang, J., 2015. A dual effect of urban expansion on flood risk in the Pearl River Delta (China) revealed by land-use scenarios and direct runoff simulation. Nat. Hazards 77, 111–128. https://doi.org/10.1007/s11069-014-1583-8.

Eastman, J.R., 2016. Manual IDRISI TerrSet: Geospatial Monitoring and Modeling System. Editora: Clark Labs da Clark University, Worcester, MA, p. 393.

EMBRAPA – Empresa Brasileira de Pesquisa Agropecuária, 2006. In: Sistema Brasileiro de Classificação de Solos, vol. 2, p. 306p. Rio de Janeiro.

Fan, F., Wang, Y., Wang, Z., 2008. Temporal and spatial change detecting (1998–2003) and predicting of land use and land cover in Core corridor of Pearl River Delta (China) by using TM and ETM+ images. Environ. Monit. Assess. 137 (2), 127–147. https://doi.org/10.1007/s10661-007-9734-y.

Geological Survey, 2018. Download GLOVIS. Available from: https://glovis.usgs.gov. (Accessed 15 April 2018).

Hamdy, O., Zhao, S., Salheen, M.A., Eid, Y.Y., 2017. Analyses the driving forces for urban growth by using IDRISI Selva models abouelreesh – aswan as a case study. Int. J. Eng. Technol. 9 (3), 226–232. https://doi.org/10.7763/ijet.2017.v9.975.

Han, H., Yang, C., Song, J., 2015. Scenario simulation and the prediction of land use and land cover change in Beijing China. Sustainability 7 (4), 4260–4279. https://doi.org/10.3390/su7044260.

Haykin, S., 2001. Redes Neurais. Porto Alegre, vol. 900. Bookman.

Hoyer, R., Chang, H., 2014. Assessment of freshwater ecosystem services in the Tualatin and Yamhill basins under climate change and urbanization. Appl. Geogr. 53, 402–416. https://doi.org/10.1016/j.apgeog.2014.06.023.

Islam, K., Rahman, MdF., Jashimuddin, M., 2018. Modeling land use change using cellular automata and artificial neural network: the case of Chunati Wildlife Sanctuary, Bangladesh. Ecol. Indicat. 88 (3), 439–453. https://doi.org/10.1016/j.ecolind.2018.01.047.

Keshtkar, H., Voigt, W., 2016. A spatiotemporal analysis of landscape change using an integrated Markov chain and cellular automata models. Model. Earth Syst. Environ. 2, 10. https://doi.org/10.1007/s40808-015-0068-4.

Landis, J.R., Koch, G.G., 1977. The measurement of observer agreement for categorical data. Biometrics 33 (1), 159–174. https://doi.org/10.2307/2529310.

Liebertrau, A.M., 1983. Measures of Association. Sage Publications. Quantitative, Newbury Park, CA, p. 1983.

Lima, A., Silva, T.S.F., de Aragão, L.E.O.C., de Feitas, R.M., Adami, M., Formaggio, A.R., Shimabukuro, Y.E., 2012. Land use and land cover changes determine the spatial relationship between fire and deforestation in the Brazilian Amazon. Appl. Geogr. 34, 239–246. https://doi.org/10.1016/j.apgeog.2011.10.013.

Lira, P.K., Tambosi, L.R., Ewers, R.M., Metzgera, J.P., 2012. Land-use and land-cover change in Atlantic Forest landscapes. For. Ecol. Manag. 278, 80–89. https://doi.org/10.1016/j.foreco.2012.05.008.

Liu, G., Jin, Q., Li, J., Li, L., He, C., Huang, Y., Yao, Y., 2017. Policy factors impact analysis based on remote sensing data and the CLUE-S model in the Lijiang River Basin, China. Catena 158, 286–297. https://doi.org/10.1016/j.catena.2017.07.003.

Mas, J.F., Kolb, M., Paegelow, M., Olmedo, M.C., Houet, T., 2014. Inductive pattern-based land use/cover change models: a comparison of four software packages. Environ. Model. Softw 51 (1), 94–111. https://doi.org/10.1016/j.envsoft.2013.09.010.
Megahed, Y., Cabral, P., Silva, J., Caetano, M., 2015. Land cover mapping analysis and urban growth modelling using Remote Sensing techniques in Greater Cairo Region – Egypt. ISPRS Int. J. Geo-Inf. 4 (3), 1750–1769. https://doi.org/10.3390/ijgi4031750.
Mendoza, M.E., Granados, E.L., Geneletti, D., Pérez-Salicrup, D.R., Salinas, V., 2011. Analysing land cover and land use change process at watershed level: a multi temporal study in the Lake Cuitzeo Watershed, Mexico (1975-2003). Appl. Geogr. 31 (1), 237–350. https://doi.org/10.1016/j.apgeog.2010.05.010.
Menezes, R., Sampaio, E., Giongo, V., Pérez-Marin, A., 2012. Biogeochemical cycling in terrestrial ecosystems of the Caatinga biome. Braz. J. Biol. 72, 643–653. https://doi.org/10.1590/S1519-69842012000400004.
Mishra, V.N., Rai, P.K., Mohan, K., 2014. Prediction of land use changes based on land change modeler (LCM) using remote sensing: a case study of Muzaffarpur (Bihar), Índia. J. Geogr. Inst. Jovan Cvijic 64 (1), 111–127. https://doi.org/10.2298/IJGI1401111M.
Monteiro Junior, J.J., Silva, E.A., Reis, A.L.A., Santos, J.P.M.S., 2018. Dynamical spatial modeling to simulate the forest scenario in Brazilian dry forest landscapes. Geol. Ecol. Landsc. https://doi.org/10.1080/24749508.2018.1481658.
Mozumder, C., Tripathi, N.K., Losiri, C., 2016. Comparing three transition potential models: a case study of built-up transitions in North-East India. Comput. Environ. Urban Syst. 59 (1), 38–49. https://doi.org/10.1016/j.compenvurbsys.2016.04.009.
Nasiri, V., Darvishsefat, A.A., Rafiee, R., Shirvany, A., Hemat, M.A., 2018. Land use change modeling through an integrated Multi-Layer Perceptron Neural Network and Markov chain analysis (case study: arasbaran region, Iran). J. For. Res. 30 (3), 943–957. https://doi.org/10.1007/s11676-018-0659-9.
Pacheco, J.D., Hewitt, R.J., 2014. Modelado del cambio de usos del suelo urbano a través de Redes Neuronales Artificiales. Comparación con dos aplicaciones de software. GeoFocus 14 (1), 1–22.
Pontius Jr., R.G., Si, K., 2014. The total operating characteristic to measure diagnostic ability for multiple thresholds. Int. J. Geogr. Inf. Sci. 28 (3), 570–583. https://doi.org/10.1080/13658816.2013.862623.
Postel, S.L., Thompson, B.H., 2005. Watershed protection: capturing the benefits of nature's water supply services. Nat. Resour. Forum 29, 98–108.
Sampaio, D.M., 2014. Modelagem da cobertura do solo urbano no Vetor Norte da RMBH e projeções de cenários futuros considerando as novas infraestruturas viárias previstas. Dissertação (Mestrado em Análise e Modelagem de Sistemas Ambientais). Universidade Federal de Minas Gerais, Belo Horizonte, p. 103.
Sano, E.E., Ferreira, L.G., Asner, G.P., Steinke, E.T., 2007. Spatial and temporal probabilities of obtaining cloud-free Landsat images over the Brazilian tropical savanna. Int. J. Remote Sens. 28 (12), 2739–2752. https://doi.org/10.1080/01431160600981517.
Santana, E.F., Vidal Batista, L., Silva, R.M., Santos, C.A.G., 2014. Multispectral image unsupervised segmentation using watershed transformation and cross-entropy minimization in different land use. GIScience Remote Sens. 51 (6), 613–629. https://doi.org/10.1080/15481603.2014.980095.
Santini, M., Caccamo, G., Laurenti, A., Noce, S., Valentini, R., 2010. A multi-component GIS framework for desertification risk assessment by an integrated index. Appl. Geogr. 30 (3), 394–415. https://doi.org/10.1016/j.apgeog.2009.11.003.
Santos, C.A.G., Brasil Neto, R.M., da Silva, R.M., Costa, S.G.F., 2019. Cluster analysis applied to spatiotemporal variability of monthly precipitation over Paraíba state using tropical rainfall measuring mission (TRMM) data. Remote Sens. 11, 637–655. https://doi.org/10.3390/rs11060637.
Santos, C.A.G., Silva, R.M., Silva, A.M., Brasil Neto, R.M., 2017. Estimation of evapotranspiration for different land covers in a Brazilian semi-arid region: a case study of the Brígida River basin, Brazil. J. South Am. Earth Sci. 74 (1), 54–66.
Schulp, C.J.E., Levers, C., Kuemmerle, T., Tieskens, K.F., Verburg, P.H., 2019. Mapping and modelling past and future land use change in Europe's cultural landscapes. Land Use Policy 80, 332–344. https://doi.org/10.1016/j.landusepol.2018.04.030.
Silva, R.M., Santos, C.A.G., Maranhão, K.U.A., Silva, A.M., Lima, V.R.P., 2018a. Geospatial assessment of eco-environmental changes in desertification area of the Brazilian semi-arid region. Earth Sci. Res. J. 22 (3), 175–186. https://doi.org/10.15446/esrj.v22n3.69904.
Silva, R.M., Santos, C.A.G., dos Santos, J.Y.G., 2018b. Evaluation and modeling of runoff and sediment yield for different land covers under simulated rain in a semiarid region of Brazil. Int. J. Sediment Res. 33 (2), 117–125. https://doi.org/10.1016/j.ijsrc.2017.04.005.
Singh, S.K., Mustak, Sk, Srivastava, P.K., Szabó, S., Islam, T., 2015. Predicting spatial and decadal LULC changes through cellular automata Markov chain models using earth observation datasets and geo-information. Environ. Process. 2 (1), 61–78. https://doi.org/10.1007/s40710-015-0062-x.
Sinha, S., Sharma, L.K., Nathawat, M.S., 2015. Improved Land-use/Land-cover classification of semi-arid deciduous forest landscape using thermal remote sensing. Egypt. J. Remote Sens. Space Sci. 18 (2), 217–233. https://doi.org/10.1016/j.ejrs.2015.09.005.
Soares-Filho, B., Rodrigues, H., Follador, M., 2013. A hybrid analytical-heuristic method for calibrating land-use change models. Environ. Model. Softw 43 (1), 80–87. https://doi.org/10.1016/j.envsoft.2013.01.010.
Sousa, F.P., Ferreira, T.O., Mendonça, E.S., Romero, R.E., Oliveira, J.G.B., 2012. Carbon and nitrogen in degraded Brazilian semi-arid soils undergoing desertification. Agric. Ecosyst. Environ. 148, 11–21. https://doi.org/10.1016/j.agee.2011.11.009.
Souza, B.I., Suertegaray, D.M.A., Lima, E.R.V., 2009. Desertificação e seus efeitos na vegetação e solos do Cariri Paraibano. Mercat. Fortaleza 8 (16), 217–232.
Valdivieso, F.O., Sendra, J.B., 2010. Application of GIS and remote sensing techniques in generation of land use scenarios for hydrological modeling. J. Hydrol. 395, 256–263. https://doi:10.1016/j.jhydrol.2010.10.033.
Vega, J.M., Diaz, A., Nava, J.M., Gallardo, M., Echavarría, P., 2017. Assessing land use-cover changes and modelling change scenarios in two mountain Spanish national parks. Environments 4 (4), 79–93. https://doi.org/10.3390/environments4040079.
Xavier, A.P.C., Silva, R.M., 2018. A GIS-based method for temporal dynamic modelling of the land use and land cover in the Tapacurá River basin (PE). Geociencias 37 (1), 193–210 (in Portuguese).
Zare, M., Panagopoulos, T., Loures, L., 2017. Simulating the impacts of future land use change on soil erosion in the Kasilian watershed, Iran. Land Use Policy 67 (5), 558–572. https://doi.org/10.1016/j.landusepol.2017.06.028.
Zolin, C.A., 2010. Análise e otimização de projetos de Pagamentos por Serviços Ambientais (PSA) utilizando Sistemas de Informações Geográficas (SIG)- o caso do município de Extrema, MG. Tese (Doutorado em Ciências). Universidade de São Paulo, Piracicaba.